Volume 6 | Number 11 | 21 March 2018 | Pages 2607–2890

Journal of Materials Chemistry C

Materials for optical, magnetic and electronic devices

rsc.li/materials-c

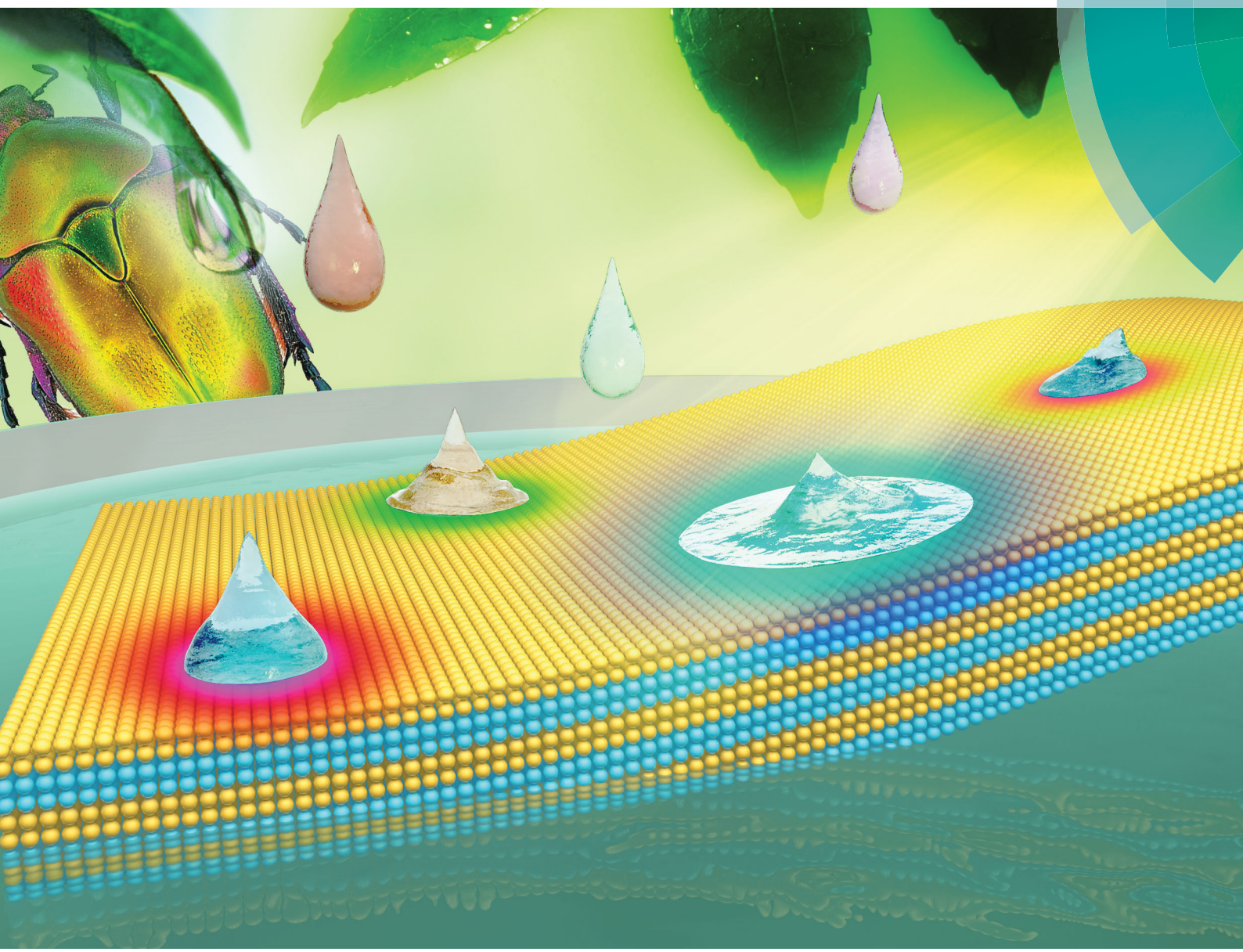

ISSN 2050-7526

ROYAL SOCIETY OF CHEMISTRY

PAPER

Wei Ma *et al.*

Porous organic/inorganic hybrid one-dimensional photonic crystals for rapid visual detection of organic solvents

Journal of Materials Chemistry C

PAPER

View Article Online
View Journal | View Issue

Cite this: J. Mater. Chem. C, 2018, 6, 2704

Porous organic/inorganic hybrid one-dimensional photonic crystals for rapid visual detection of organic solvents†

Donghui Kou,[a] Shufen Zhang,[a] Jodie L. Lutkenhaus,[bc] Lin Wang,[a] Bingtao Tang[a] and Wei Ma*[a]

Received 24th November 2017,
Accepted 4th February 2018

DOI: 10.1039/c7tc05390h

rsc.li/materials-c

Stimuli-responsive photonic crystals (PCs) recently have bloomed into a fast-growing research area arousing wide scientific enthusiasm. Here, we propose a kind of highly sensitive and simple liquid organic solvent-responsive one-dimensional photonic crystal (1DPC) sensor derived from porous poly(methyl methacrylate–acrylic acid–ethyleneglycol dimethacrylate)/titania (P(MMA–AA–EGDMA)/TiO_2) with structural colors. These organic/inorganic hybrid 1DPCs with textural porosity are fabricated through layer-by-layer assembly based on spin-coating of a microemulsion of polymer nanoparticles and a suspension of TiO_2 nanoparticles on silicon substrates. The larger refractive index contrast allows the desired reflectivity to be achieved with a few layers of the 1DPCs. Tunable optical properties of the 1DPC sensors are achieved by modulating the nanoparticle concentration, rotational speed, spin-coating times and stack number. The solvent tunability of the sensors is due to the dependence of the layer refractive index and thickness of the 1DPCs on solvents. Notably, owing to the porosity generated from the nanoparticle-based structure and the high sensitivity of the crosslinked polymer nanoparticles to organic solvents, the obtained 1DPCs present a rapid (within 2 s), obvious and distinguishable color change when immersed in different organic solvents, and the visual detection process shows good reversibility. In addition, the 1DPC sensors also show different responses to various concentrations of organic solvents in water, such as ethanol, methanol and acetone. The porous organic/inorganic hybrid 1DPCs offer high potential for the development of economical and visually detective solvent sensors with high performance.

Introduction

Organic solvents, one of the most common and important chemical agents, play a crucial role in the chemical industry,[1] food industry,[2] biotechnology,[3] medical research[4] and so on. They are a major convenience for industries, however, causing much inconvenience when released.[5] As we all know, the majority of the industrial processes relating to organic solvents pose threats to human health and the environment.[6] Organic solvents not only pollute the air environment in the gas form[7] but also result in long-term adverse effects on the aquatic environment.[8] As a traditional and common technique for solvent detection, gas chromatography-mass spectrometry (GC-MS) regrettably suffers from time-consuming, complicated operation procedures, and expensive and heavy devices.[9,10] At present, many different organic solvent detectors have been developed, including solvatochromic fluorescence probes,[11] electronic nose,[12] quartz crystal microbalance (QCM),[13] photonic crystals (PCs)[14] and solvent-response structures materials.[15–17] Among them, PCs, which comprise of the periodic nanostructures of two dielectric components, have attracted scientists' significant attention and enthusiasm. The periodic arrangement of the dielectric constituents endows the PCs with a property known as the photonic band gap (PBG). The visual solvent tunability of the PCs is based on the tunable PBG within the visible region owing to solvent-responsive structures, including the responsive refractive index or the thickness of the PCs.

1DPCs, which are derived from an alternating assembly of materials with high and low refractive indexes, are the simplest members in the PC family.[18] They show the characteristics of wide material selection,[19–21] good stability,[22] and have been demonstrated to be of high value in organic solvent detection

[a] State Key Laboratory of Fine Chemicals, Dalian University of Technology, Dalian, Liaoning 116023, P. R. China. E-mail: weima@dlut.edu.cn; Tel: +86-411-84986506
[b] Artie McFerrin Department of Chemical Engineering, Texas A&M University, College Station, Texas 77843, USA
[c] Department of Materials Science and Engineering, Texas A&M University, College Station, Texas 77843, USA

† Electronic supplementary information (ESI) available. See DOI: 10.1039/c7tc05390h

through variation of both the refractive index and layer thickness based on the Bragg equation.[23] It was reported that porous SiO_2/TiO_2[24,25] and layered double hydroxide (LDH)/TiO_2[26] 1DPCs have been used as sensors for organic solvents. The optical response of these inorganic sensors is owing to the change of refractive index through the penetration of solvents into mesopores within the inorganic material layers. Unfortunately, since there is only a small distinction among the refractive indexes of some solvents, the color change is not very distinguishable for the solvents.

Some polymers are very sensitive to organic solvents, their introduction to 1DPCs will increase the solvatochromic effect through the swelling of the polymer layers, which is beneficial for producing high-performance sensors. In this respect, organic/inorganic hybrid 1DPCs have attracted much attention as solvent sensors. They also show the advantage of possessing a large refractive index contrast for producing brilliant structural colors with only a few alternating layers.[27–29] An organic/inorganic hybrid 1DPC film consisting of poly(1,2-butadiene) (PB) and osmium (Os) multi-layers was reported to show obvious change in the position of the reflection peaks on swelling the PB layers with hexane.[30] In a similar way, poly(methyl methacrylate–hydroxyethyl methacrylate–ethylene glycol dimethacrylate) P(MMA–HEMA–EGDMA)/TiO_2 1DPC was fabricated for solvent detection.[31] The polymer layers were continuous compact films assembled by the spin-coating of P(MMA–HEMA–EGDMA) in butanone. The response process reaches a balance within 2 min for most solvents mainly through swelling of the polymer layer to different degrees.[31]

In this paper, aiming to obtain much more efficient solvent-responsive 1DPC sensor, organic/inorganic hybrid 1DPCs with textural porosity were constructed with an aqueous-based layer-by-layer assembly of a microemulsion of poly(methyl methacrylate–acrylic acid–ethyleneglycol dimethacrylate) (P(MMA–AA–EGDMA)) nanoparticles and a suspension of TiO_2 nanoparticles on silicon substrates. The assembly procedure and sensing mechanism are shown in Fig. 1a and b, respectively. It can be observed that an inherent and accessible porosity is formed from the nanoparticle-based assembly, which is essential for effective solvent infiltration and sensing. The polymer and TiO_2 are selected as the low (n_l) and high (n_h) refractive index materials, respectively, and the large refractive index contrast of these materials is beneficial for obtaining a brilliant color with only a few stacks, which is important for the easy recognition of color change when the 1DPC sensors receive external stimuli. PMMA, which is very sensitive to organic solvents is designed as the main component of the polymer layer, the AA addition can increase hydrophilicity and benefit the assembly with a titania layer, and EGDMA was used as the crosslinker to realize the high stability of the copolymer in liquid solvents.

In our previous work,[32] a nanoparticle-based P(MMA–AA)/TiO_2 1DPC was designed and constructed for realizing environmentally friendly assembly and easily achieving a discrete layer interface. The 1DPC was preliminarily used for the organic solvent vapor response and showed good sensitivity and repeatability. However, the obtained 1DPCs were very unstable in liquid organic solvents.

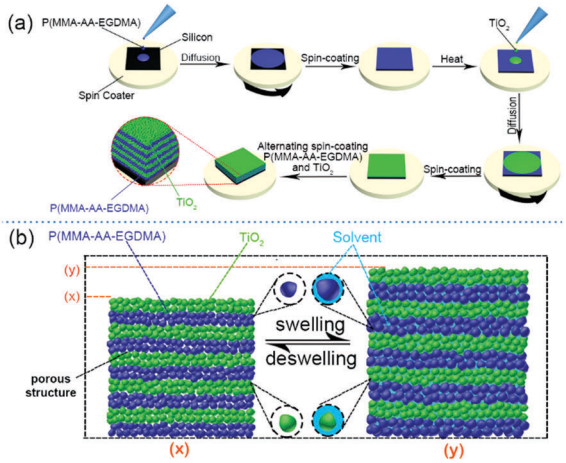

Fig. 1 (a) Schematic of fabrication of P(MMA–AA–EGDMA)/TiO_2 1DPCs with structural colors *via* the layer-by-layer spin-coating process; (b) the illustration of 1DPC swelling and deswelling in an organic solvent: (x) original 1DPC; (y) the 1DPC soaked in organic solvent.

Based on a previous study, we for the first time design a highly efficient liquid organic solvent sensor derived from a porous organic/inorganic hybrid 1DPC. Through the appropriate dosage of the crosslinker EGDMA in the microemulsion system, P(MMA–AA–EGDMA) with an average diameter of 44.4 nm was successfully prepared and showed very good stability in all common organic solvents. In this study, the optical properties of the prepared solvent sensors were investigated by changing the processing parameters in spin-coating including the concentration of TiO_2, rotational speed, spin-coating times, and stack number. The color change sensitivity, PBG shift and reversibility of the 1DPC sensor for various organic solvents, including carbon tetrachloride (CTC), ethanol (EA), ethyl acetate (EAC), methylene chloride (DCM), chloroform (TCM) and other solvents were studied and the sensing mechanism is discussed. Moreover, this new sensor was employed to detect the aqueous solutions of certain solvents, such as ethanol, methanol and acetone, and the visually detective properties were also examined and discussed to comprehensively evaluate the 1DPCs as a kind of sensitive and simple solvent sensor.

Experimental

Materials

Methyl methacrylate (MMA, 99.5%) and acrylic acid (AA, 99.0%) were purchased from Tianjin Bodie Chemical Co., Ltd. Ethyleneglycol dimethacrylate (EGDMA, 98%) was purchased from Aladdin Industrial Corporation (Shanghai, China) and purified before use. Anatase nano titania (TiO_2) was purchased from Xuancheng Jingrui New Materials Company. All the solvents and other chemicals were supplied by local suppliers. Silicon wafers (100) were cut into 20 mm × 20 mm pieces and pretreated by first immersing them in a solution containing H_2O_2 (30%)/ammonia water (25%)/deionized water (volume ratio of 5 : 1 : 1), and then the solution was heated to 70 °C

and kept at the same temperature for 15 min. After that, the silicon wafers were washed with deionized water and dried.

Preparation of the polymer microemulsion and TiO_2 sol

Polymer nanoparticles were synthesized *via* a modified microemulsion polymerization.[32,33] 10.0 g MMA, 1.0 g AA and 1.5 g EGDMA were first mixed uniformly. Then 2.5 g of the above mixed monomers, 0.67 g cetyl trimethyl ammonium bromide and 50.0 mL water were added to a 150 mL flask equipped with an addition funnel, a reflux condenser, a stirrer and a nitrogen entry port, and the mixture was heated to 75 °C for 20 min under nitrogen. Then 33.0 mg potassium persulfate dissolved in 5.0 mL water was added into the above flask. The polymerization proceeded for 30 min. After that, the remainder of the mixed monomers was added dropwise to the polymerizing system within 1.0 h. Then the reaction was kept at 75 °C for another 30 min. When the polymerization was finished the product was cooled down to room temperature. Finally, the prepared P(MMA–AA–EGDMA) microemulsion was diluted to the appropriate concentration with water before use. The TiO_2 dispersion was made by dispersing a certain amount of TiO_2 power into a mixture of ethanol/deionized water (volume ratio of 1 : 1).

Fabrication of 1DPC sensors

1DPC sensors were prepared by alternately spin-coating the polymer microemulsion (5 wt%) and TiO_2 sol (1 wt%, 2 wt% or 3 wt%) onto silicon wafers with a spin coater (Laurell WS-650SZ-6NPP/LITE). The polymer layer was the first layer just next to the silicon substrate, and the TiO_2 layer was the top layer on the surface of the film in the whole preparation process. The layers were dried at 60 °C for 60 s after the one-layer assembly. Finally, the obtained 1DPC sensors were rinsed with acetone and ready for use.

Characterization of 1DPC sensors

SEM micrographs of 1DPCs were recorded with an Ultra-High Resolution Scanning Electron Microscope (SEM) of the SU8200 series. The average particle diameter and particle size distribution of the polymer and TiO_2 nanoparticle were recorded using dynamic light scattering spectroscopy (Zetssizer 1000, Malvern, UK). The refractive indexes of P(MMA–AA–EGDMA) and TiO_2 layers were measured by an Ellipsometer type Ellip-ER-III under a certain wavelength (632.8 nm). The reflectance spectra of the samples (incident angle of 15°), which ranged from 350 to 800 nm, were obtained by using a HITACHI U-4100 spectrophotometer at a scan speed of 300 nm min^{-1}. A Nikon digital camera was used for capturing (at 15°) the optical photos of the 1DPCs.

Organic solvent response

Organic solvent responsive tests of 1DPC sensors were implemented by immersing the samples in organic solvents of *n*-hexane (HEX), CTC, diethyl ether (DEE), acetonitrile (ACN), EA, EAC, DCM, and TCM, respectively. The 1DPC films were immersed into organic solvents and the photographs of the 1DPC sensors were captured after 2 s of soaking in the solvents. The reflection spectra of the sensors were measured after 2 s of immersion in solvents, and after being taken out of the solvents and dried. The above experimental process was repeated many times to evaluate the reversibility of the sensors.

Results and discussion

1DPC sensor preparation and structural properties

For the assembly of porous 1DPC films, the particle size should be controlled in the range of 5 nm to 50 nm, and a good particle dispersing property is an important factor to decrease the imperfections in the deposited layer. Otherwise, it is difficult to form smooth layers and achieve good optical properties.[34] Microemulsion polymerization is an effective method to prepare polymer nanoparticles with an average diameter lower than 100 nm.[35,36] In this study, the polymer nanoparticles were successfully synthesized using a modified microemulsion polymerization.[32,33] Based on the experimental results, it was found that a mass ratio of MMA, AA and EGDMA of 10 : 1 : 1.5 was good for obtaining the crosslinked polymer nanoparticles with a suitable particle size and superior organic solvent stability. Too much or too little crosslinker will result in the formation of a large polymer gel or inferior solvent resistance, respectively, which cannot satisfy the assembly and application requirements.

The SEM images of the polymer in Fig. 2a and TiO_2 in Fig. 2b show that the shapes of both the polymer and the TiO_2 are nanoparticles. The spheres are P(MMA–AA–EGDMA) nanoparticles whereas the smaller particles are TiO_2 nanocrystallines. Their average particle diameters and particle size distributions are shown in Fig. S1 (ESI†). It was shown that the average diameters of the polymer and TiO_2 nanoparticles are 44.4 nm and 35.3 nm, respectively. In addition, the prepared polymer microemulsion shows good stability under weakly acidic and neutral conditions at room temperature (see Fig. S2, ESI†).

The 1DPC sensors were assembled by alternately spin-coating the polymer microemulsion twice and the TiO_2 suspension (3 wt%) three times. Fig. 2c presents the cross-sectional SEM image and digital photography of a green 1DPC film consisting of five bilayers. A distinct multilayered structure of 1DPC could be observed while the TiO_2 layers and polymer layers can be recognized easily because the TiO_2 layers are brighter owing to their higher electron density.

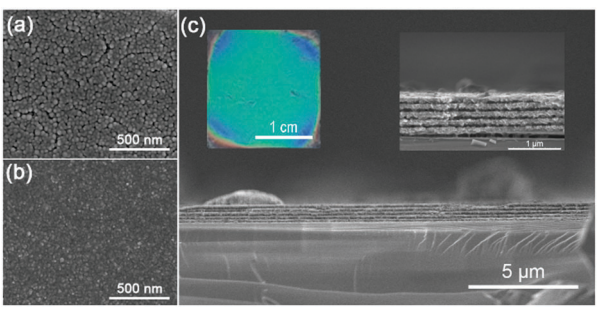

Fig. 2 (a) SEM images of polymer nanoparticles; (b) SEM images of TiO_2 nanoparticles; (c) digital photograph and cross-sectional SEM images of a 5-stack 1DPC.

The thickness of the polymer and TiO_2 layers are measured to be about 63 nm and 100 nm, which corresponds to approximately one polymer nanoparticle and three TiO_2 nanoparticles, respectively. Furthermore, in Fig. 2c, the enlarged cross-sectional image shows the nanoparticle characteristics of the 1DPC sensor. It was calculated that the porosity of the polymer and TiO_2 layers was 20.8% and 34.2%, respectively, utilizing a recently reported method based on ellipsometry.[37] In addition, it is measured that the refractive indices of the P(MMA–AA–EGDMA) and TiO_2 layers are 1.375 and 1.775, respectively. Thanks to the refractive index contrast, a distinct PBG is attained in only several stacks and the digital photography in Fig. 2c shows a bright green color.

Optical properties of the 1DPC sensors

The optical properties, including the position of the reflection peak, and the peak intensity were investigated in this study. These properties were modulated through varying the layer thickness and stack number. The first-order reflection wavelength of a 1DPC can be predicted by Bragg's law (1)[38] and the maximum Bragg peak intensity is given by the following expression (2):[38]

$$\lambda_{max} = 2(n_l d_l + n_h d_h) \quad (1)$$

$$R = \left(\frac{1-Y}{1+Y}\right)^2 \times 100\%, \quad Y = \left(\frac{n_h}{n_l}\right)^{N-1} \frac{n_h^2}{n_s} \quad (2)$$

where λ_{max} is the position of the first-order refraction wavelength, d_h and d_l are the thickness of the high- and low-refractive-index regions, n_s is the refractive index of the substrate, n_h and n_l are the refractive indices of the high- and low-index regions, respectively, N is the number of periods of the 1DPCs. From the above formula, the first-order refraction wavelength can be modulated by varying the layer thickness and refractive indices, and the reflectivity is enhanced with the increase in both n_h/n_l and the number of the periods.

According to eqn (1), by varying the layer thickness, the position of the reflection peak can be turned and different structural colors are achieved. The structural colors and reflectance spectra of the 1DPC sensors are summarized in Fig. 3. The layer thicknesses were manipulated by changing the assembly concentration of TiO_2 (Fig. 3a), spin-coating speed (Fig. 3b) and spin times of TiO_2 (Fig. 3c). In Fig. 3a, keeping the spin speed at 3000 rpm and the spin-coating twice of the TiO_2 sol for each layer, it was shown that with the mass fraction of TiO_2 increase from 1% to 2%, then to 3%, the color of the 1DPCs turned from purple to blue, then to yellow-green, and the first-order reflected wavelength changed from 403 nm to 458 nm, and then to 494 nm, respectively. And in Fig. 3b, keeping the mass fraction of TiO_2 at 2% and the spin-coating twice for each layer, it shows that when the spin-coating speed increased from 3000 rpm to 4000 rpm, and then to 5000 rpm, the layer thickness decreased gradually leading to a color change from blue-green to dark blue, and then to purple, respectively and a blue shift of the position of the reflection peak from 507 nm to 438 nm, and then to 391 nm, respectively. The thickness of TiO_2 layer can also increase by increasing the TiO_2 (2%) spin-coating times as shown in Fig. 3c. By keeping the spin-coating speed constant

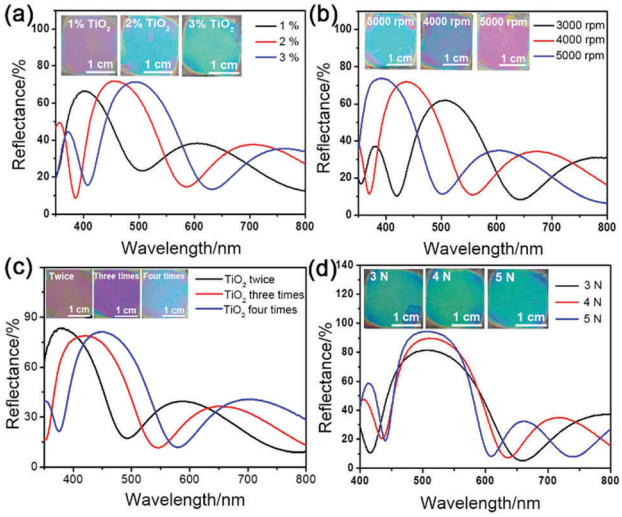

Fig. 3 Structural colors and reflectance spectra of sensors with different (a) TiO_2 concentrations; (b) spinning speed; (c) TiO_2 times (d) numbers of Bragg stacks.

at 4000 rpm, the spin-coating times of TiO_2 increased from twice to three times, and then to four times, the maximum reflection wavelength of the 1DPC with lavender color changed from 378.5 nm to 419.5 nm, and then to 449.5 nm and accordingly its color turned from lavender to dark violet, and then to blue, respectively.

Fig. 3d gives the effect of the Bragg stack number on the reflectance spectra and the structural colors. Green 1DPC films with various stack numbers were assembled and their Bragg reflection peaks all located at around 510 nm. It can be observed that on increasing the stack number from 3 to 5, the color of the 1DPCs became gradually brighter and the peak intensity increased from 81.60% to 94.53%. This phenomenon can be theoretically described according to eqn (2). Also, by increasing the Bragg stack number, the bandwidth became narrower, this is also described in the other ref. 39 and 40.

As is clear from the above descriptions, the 1DPCs prepared in this way have the universal optical properties of Bragg stacks.

Response of 1DPCs toward organic solvents

A 3-stack 1DPC was prepared by alternatively spin-coating TiO_2 sol (3 wt%) twice and the polymer microemulsion twice at 3000 rpm. The colorimetric response of the 1DPC sensor towards various solvents was explored by directly comparing the color and monitoring its reflectance spectra in different solvents. As shown in Fig. 4a, the 1DPC sensor with a violet color was immersed into the organic solvents of CTC, EA, EAC, DCM and TCM, respectively; the color of the sensor changes very quickly, within 2 s from violet to blue, yellow, orange, orange-red and black red, respectively, and the maximum reflection wavelength shifts from the original 437 nm to 471 nm, 556 nm, 601 nm, 645 nm and 682 nm, respectively (Fig. 4b). For all the solvents tested, the responsive process reaches a balance in 2 s and the reflection peaks of the sensor in DCM and acetone have been recorded with different response times (Fig. S3, ESI†). In Fig. 4c, the color coordinate

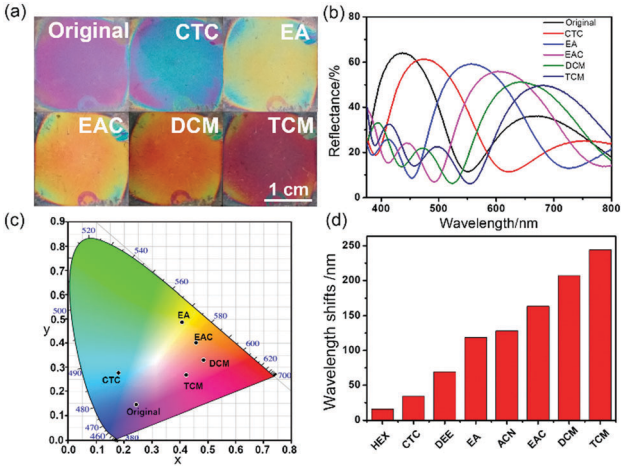

Fig. 4 (a) Photographs of the 1DPC sensor in different solvents; (b) reflectance spectra of the sensor in various solvents; (c) CIE 1931 chromaticity coordinates of the sensor in various solvents; (d) shifts of the photonic stop band of the sensor in various solvents.

also turns from violet (CIE: (0.2431, 0.1444)) to blue (CIE: (0.1800, 0.2767)), yellow (CIE: (0.4072, 0.4868)), orange (CIE: (0.4582, 0.4008)), orange-red (CIE: (0.4848, 0.3287)) and finally black red (CIE: (0.42292, 0.2683)), respectively, which is in line with the colors of the 1DPCs in the different solvents mentioned above. Due to existence of mesopores and the solvent-sensitive polymer, the sensor became very sensitive to the solvents, and an obvious and distinguishable color change was observed, indicating the 1DPC is suitable for the visual detection of organic solvents.

It can be observed from the reflectance spectra (Fig. 4b) that with the spectra shifting to a longer wavelength, the reflectivity decreases and bandwidth increases. This could result from the variation of the relative index contrast on account of the infiltration of solvents into the multilayer.[31]

According to Bragg equation (1), a bathochromic shift of the maximum reflection wavelength can be realized by increase of the refractive index or the layer thickness, or the increase in both. Accordingly, the bathochromic shift of the reflection wavelength in Fig. 4 is related to an increase in refractive index or layer thickness.[22,41] Since the nanoparticle-based 1DPC sensor contains abundant mesopores, solvent compounds could enter it much easily through capillarity and replace the air within the mesopores accordingly, which caused an increase in the refractive indices of both layers, and then a stopband red shift. However, it is found that the difference in the refractive indices of the organic solvents is not large, for example, n_{CTC} = 1.46, n_{EA} = 1.36, n_{EAC} = 1.37, n_{DCM} = 1.42 and n_{TCM} = 1.44. These could not individually cause such a distinct difference in reflectance spectra and color for various solvents. The increase in the polymer layer thickness through solvent swelling is an important reason for the obvious and distinguishable shift of the photonic band stop. From the literature, the swelling degree of solvents to polymers is mainly determined by the three dimension solubility parameters which arise from the dispersion forces (δ_d), permanent dipole–permanent dipole forces (δ_p) and hydrogen bonding (δ_H).[42]

If the solubility parameters for the polymers and solvents are very close to each other, the polymers show good miscibility with the solvents.[43] Thus if the polymer is crosslinked to form a gel, the swelling degree of the crosslinked polymer is larger accordingly. It was reported that the solubility parameter of PMMA which is the main constituent of polymer nanoparticles is 9.19 ($cal^{1/2}$ $cm^{-3/2}$)[44] and the solubility parameters of CTC, EA, EAC, DCM and TCM are 8.65, 12.98, 9.07, 9.9 and 9.22, respectively. The solubility parameter value of TCM (9.22) is the closest one to that of PMMA (9.19), and TCM has a relatively large refractive index of 1.44, thus the color change and shift of the maximum reflection wavelength are the biggest in the presence of TCM as shown in Fig. 4a and b, respectively. The solubility parameter of EAC is a little closer to that of PMMA compared with that of DCM, while the refractive index of EAC (n = 1.37) is lower than that of DCM (n = 1.42). Due to the combined reasons of solubility parameter and refractive index of the solvents, the change in color and the maximum reflection wavelength of the sensor in EAC is smaller than that in DCM as presented in Fig. 4a and b, respectively. For CTC and EA, it is found that the solubility parameter of CTC is closer to that of PMMA, and CTC also has larger refractive index compared with that of EA. However, the influence of EA on the change in color and reflection spectrum is much larger than that of CTC as shown in Fig. 4. This can be illustrated by the swelling ability of EA to the crosslinked PAA which is another component of the copolymer. In addition, EA has a larger polarity which results in better affinity to the hydrophilic TiO_2 layer. Besides these five solvents, the other solvents were also compared (Fig. 4d) and showed that other factors except solubility parameter and refractive index of solvents also make a difference in the swelling degree of the polymer. For instance, compared with DEE (δ_p: 1.4), the solubility parameter of CTC (δ_p: 0) is closer to that of PMMA, nonetheless, as the polarity of DEE becomes higher, the shift of the PBG of the sensor in DEE becomes bigger than that in CTC as other studies have reported[31] according to the well-known "like dissolve like" aphorism.[45]

As diverse interactions and influential factors exist between the 1DPC sensor and different solvent molecules, the layer thickness and refractive index of the sensor show distinguishable variations, which generate different optical properties for solvent detection.

In order to confirm the swelling of the polymer in an organic solvent, the particle size of P(MMA–AA–EGDMA) was measured in both water and ethanol using dynamic light scattering spectroscopy (see Fig. 5). The average particle diameter of the polymer nanoparticles in water is 44.4 nm, while the average particle diameter of polymer nanoparticles in ethanol is 97.7 nm. The increase in the average diameter of the polymer nanoparticles confirms the swelling of the polymer of the sensor in ethanol. In addition, the thicknesses of TiO_2 layer and polymer layer are measured in air and solvent using an ellipsometer, respectively. The thicknesses of the TiO_2 film are about 66.78 nm and 65.63 nm before and after soaking in ethanol, respectively, indicating the TiO_2 layer remains unchanged in ethanol. Nevertheless, the thicknesses of a one-stack 1DPC film, which consists of one TiO_2 layer and one polymer layer, are approximately 93.23 nm and 122.66 nm before

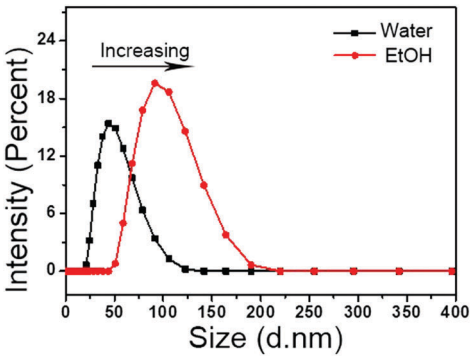

Fig. 5 Particle size distribution (vol%) of the polymer nanoparticle micro-emulsion in water and ethanol.

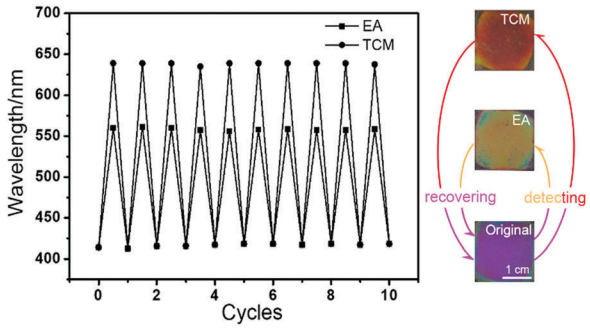

Fig. 6 Recycle detection test of the 1DPC sensor in ethanol and chloroform.

and after soaking in ethanol, respectively. These results demonstrate the swelling of the polymer layer in ethanol, which results in an increase in polymer thickness and a red-shift of the PBG.

Moreover, good repeatability is also an important property for a practical sensor. Fig. 6 shows ten cycle responsive tests of a 1DPC for ethanol and chloroform detection, respectively. The position of the reflection peak reversibly turned from the original 417 nm to 558 nm and 639 nm, respectively, and the color accordingly transforms from violet to yellow and black red, respectively. This demonstrates that the P(MMA–AA–EGDMA)/TiO_2 1DPC sensor with crosslinked polymer possesses a satisfactory reversibility. Furthermore, the porous structure could be maintained after repeated use for solvent detection, as shown in Fig. S4 (ESI†), demonstrating the good stability of the 1DPC sensor.

Response of 1DPCs toward the organic solvent/water solution

Besides pure organic solvents, binary mixtures of organic solvent and water could also be discriminated within 2 s using this simple porous organic/inorganic hybrid 1DPC sensor. Fig. 7 shows that the 1DPC could be used to detect different concentrations of ethanol aqueous solution. Fig. 7a gives images of the colors of a 1DPC in mixtures of ethanol and water. From the figure, we can see that the colors vary from original yellow-green to magenta and then to yellow gradually with the increase of the volume fraction of ethanol from 0 to 60%–75%, and then to 100%. Theoretically, the photonic stop band changes to a longer wavelength with the increase of ethanol concentration since ethanol swells the polymer much more compared to water

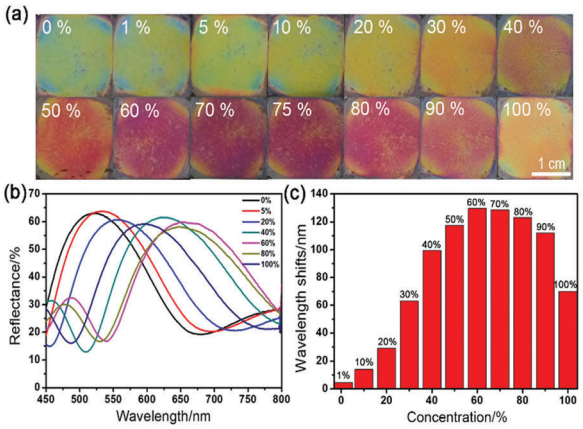

Fig. 7 (a) Photographs of the solvent sensor in alcohol solutions of different concentrations; (b) reflective spectra of the sensor in alcohol solutions of different concentrations; (c) shifts of the photonic stop band of the sensor in alcohol solutions of different concentrations.

according to the solubility parameter of ethanol (δ: 12.98) and water (δ: 23.43). However, Fig. 7b and c show that with the increase of ethanol concentration, the shift of the maximum reflection wavelength increased first and then decreased, and the shift reaches a maximum when the ethanol concentration is about 70%. Fig. S5 (ESI†) also gives the ten responsive cycles of a 1DPC sensor immersed in 60% ethanol aqueous solution which suggests the good reversibility of the 1DPC sensor in this binary mixture of ethanol and water. Moreover, methanol and acetone, which have good solubility in water also exhibit the same rule as ethanol (in Fig. S6, ESI†), namely the extent of color change increases first and then decreases with increase of solvent concentration.

The unusual swelling behavior in that the extent of swelling in mixed solvents is larger than that in pure solvents could be explained by the "cosolvency" effect.[46,47] Cosolvency of a polymer is a phenomenon wherein two "bad" solvents of the polymer act as a "good" solvent when mixed in a certain ratio. The mechanism can be qualitatively understood based on the Flory–Huggins theory.[48,49] The cosolvency phenomenon of PMMA in alcohol/water mixed solution has also been reported.[47,50] Pure ethanol and pure water are not considered as solvents for PMMA, while their cosolvent mixture within a suitable range of alcohol–water ratios form good solvents for PMMA. The cross-linked PMMA shows re-collapsing swelling behavior in the mixed solution due to the cosolvency phenomenon, indicating a good consistency between the dissolving property of PMMA and the swelling behavior of its cross-linked product in the mixed solvents. Besides the crosslinked PMMA, the PAA gel was also reported to show a bell-shape swelling curve due to the "cosolvency" effect.[51] The AA monomer consists of two parts: the hydrophilic carboxylic acid group which is weakly charged at neutral conditions and more familiar with water than ethanol, and the hydrophobic ethylene backbone has a higher solubility in ethanol than in water. Thus in a low concentration of ethanol, carboxylic acid groups play the leading role to swell the polymer nanoparticles, while the ethylene backbone of AA plays a decisive role in swelling of the 1DPC sensor

when the concentration of ethanol is high. The above mentioned can be used to illustrate the swelling behavior of P(MMA–AA–EGDMA), and the "cosolvency" effect occurred when the mixtures were prepared within a particular range of ethanol-water ratios. Accordingly, the 1DPC sensor containing the sensitive polymer shows a nonmonotonic peak shift by increasing the ethanol concentration in ethanol–water mixture solvents.

Conclusions

We demonstrate an aqueous-based and facile method to prepare solvent-responsive porous P(MMA–AA–EGDMA)/TiO_2 1DPC sensors by a layer-by-layer spin-assisted assembly. By changing different preparation parameters, these organic/inorganic hybrid 1DPCs with various structural colors were obtained. Since the 1DPC sensors possess an inherent porosity and a solvent-sensitive polymer, they show a very high response speed for all the tested solvents, the detection is accomplished within 2 s. All common organic solvents can be discriminated using this 1DPC sensor and the solvents can be visually detected through color change. Besides the use as a sensor to detect pure solvents, the 1DPC sensor can also be used as a simple device to distinguish the different concentrations of the aqueous solutions of certain organic solvents. As the 1DPC sensors can be fabricated with a simple, low-cost and environmentally friendly approach, and show a rapid, sensitive and reversible solvent response, they are promising as economical optical sensors to realize visual detection in chemical and biological fields.

Conflicts of interest

There are no conflicts to declare.

Acknowledgements

This work was financially supported by the National Natural Science Foundation of China (21376042, 21536002, and 21421005), the Program for Changjiang Scholars and Innovative Research Team in the University (IRT-13R06). This material is based in part upon work supported by the National Science Foundation of the United States (1049706).

Notes and references

1 H. L. Li, L. X. Chang, J. X. Wang, L. M. Yang and Y. L. Song, *J. Mater. Chem.*, 2008, **18**, 5098–5130.
2 M. E. Franke, T. J. Koplin and U. Simon, *Small*, 2006, **2**, 36–50.
3 G. Espinosa-Luna, M. G. Sánchez-Otero, R. Quintana-Castro, R. E. Matus-Toledo and R. M. Oliart-Ros, *Mol. Biotechnol.*, 2016, **58**, 37–46.
4 J. A. Bull, R. A. Croft, O. A. Davis, R. Doran and K. F. Morgan, *Chem. Rev.*, 2016, **116**, 12150–12233.
5 E. C. Cho, Y. S. Hsiao, K. C. Lee and J. H. Huang, *RSC Adv.*, 2015, **5**, 53741–53748.
6 M. R. Li, P. F. Harten and H. Cabezas, *Ind. Eng. Chem. Res.*, 2002, **41**, 5867–5877.
7 J. Yoon, S. K. Chae and J. M. Kim, *J. Am. Chem. Soc.*, 2007, **129**, 3038–3039.
8 G. D. Liang, F. Ren, H. Y. Gao, Q. Wu, F. M. Zhu and B. Z. Tang, *ACS Sensors*, 2016, **1**, 1272–1278.
9 C. M. Lu, S. Q. Liu, J. Q. Xu, Y. J. Ding and G. F. Ouyang, *Anal. Chim. Acta*, 2016, **902**, 205–211.
10 R. Lu, W. W. Li, B. Mizaikoff, A. Katzir, Y. Raichlin, G. P. Sheng and H. Q. Yu, *Nat. Protoc.*, 2016, **11**, 377–386.
11 J. Do, J. Huh and E. Kim, *Langmuir*, 2009, **25**, 9405–9412.
12 F. Röck, N. Barsan and U. Weimar, *Chem. Rev.*, 2008, **108**, 705–725.
13 M. Harbeck, D. D. Erbahar, I. Gürol, E. Musluoğlu, V. Ahsen and Z. Z. Öztürk, *Sens. Actuators, B*, 2010, **150**, 346–354.
14 G. B. Huang, Y. B. Yin, Z. Pan, M. X. Chen, L. Zhang, Y. Liu, Y. L. Zhang and J. P. Gao, *Biomacromolecules*, 2014, **15**, 4396–4402.
15 L. L. Gong, X. F. Feng, F. Luo, X. F. Yi and A. M. Zheng, *Green Chem.*, 2016, **18**, 2047–2055.
16 A. Toncheva, B. Willocq, F. Khelifa, O. Douheret, P. Lambert, P. Dubois and J. M. Raquez, *J. Mater. Chem. B*, 2017, **5**, 5556–5563.
17 Q. Fu, H. B. Zhang, Z. M. Wang and M. Chiao, *J. Mater. Chem. B*, 2017, **5**, 4025–4030.
18 H. Y. Xuan, J. Y. Ren, Y. X. Zhu, B. Zhao and L. Q. Ge, *RSC Adv.*, 2016, **6**, 36827–36833.
19 W. Cheng, T. Gorishnyy, V. Krikorian, G. Fytas and E. L. Thomas, *Macromolecules*, 2006, **39**, 9614–9620.
20 D. P. Puzzo, L. D. Bonifacio, J. Oreopoulos, C. M. Yip, I. Manners and G. A. Ozin, *J. Mater. Chem.*, 2009, **19**, 3500–3506.
21 B. V. Lotsch and G. A. Ozin, *Adv. Mater.*, 2008, **20**, 4079–4084.
22 C. H. Liu, C. Yao, Y. X. Zhu, J. Y. Ren, K. Lan, H. Peng and L. Q. Ge, *RSC Adv.*, 2014, **4**, 27281–27285.
23 V. Morandi, F. Marabelli, V. Amendola, M. Meneghetti and D. Comoretto, *Adv. Funct. Mater.*, 2007, **17**, 2779–2786.
24 Y. S. Choi, M. Mamak, G. V. Freymann, N. Chopra and G. A. Ozin, *Nano Lett.*, 2006, **6**, 2456–2461.
25 S. Colodrero, M. Ocaña and H. Míguez, *Langmuir*, 2008, **24**, 4430–4434.
26 Y. B. Dou, J. B. Han, T. L. Wang, M. Wei, D. G. Evans and X. Duan, *J. Mater. Chem.*, 2012, **22**, 14001–14007.
27 Z. Y. Wang, J. H. Zhang, Z. H. Wang, H. Z. Shen, J. Xie, Y. F. Li, L. Lin and B. Yang, *J. Mater. Chem. C*, 2013, **1**, 977–983.
28 C. Yao, J. Y. Ren, C. H. Liu, T. Yin, Y. X. Zhu and L. Q. Ge, *ACS Appl. Mater. Interfaces*, 2014, **6**, 16727–16733.
29 S. J. Jeon, M. C. Chiappelli and R. C. Hayward, *Adv. Funct. Mater.*, 2016, **26**, 722–728.
30 H. Yabu, T. Nakanishi, Y. Hirai and M. Shimomura, *J. Mater. Chem.*, 2011, **21**, 15154–15156.
31 Z. H. Wang, J. H. Zhang, J. X. Li, J. Xie, Y. F. Li, S. Liang, Z. C. Tian, C. Li, Z. Y. Wang, T. Q. Wang, H. Zhang and B. Yang, *J. Mater. Chem.*, 2011, **21**, 1264–1270.
32 L. Wang, S. F. Zhang, J. L. Lutkenhaus, L. Chu, B. T. Tang, S. Li and W. Ma, *J. Mater. Chem. C*, 2017, **5**, 8266–8272.
33 P. Xu, W. Zhong, H. T. Wang, R. Tong and Q. G. Du, *Colloid Polym. Sci.*, 2004, **282**, 1409–1414.
34 M. E. Calvo, S. Colodrero, N. Hidalgo, G. Lozano, C. López-López, O. Sánchez-Sobrado and H. Míguez, *Energy Environ. Sci.*, 2011, **4**, 4800–4812.

35 D. C. Steytler, A. Gurgel, R. Ohly, M. Jung and R. K. Heenan, *Langmuir*, 2004, **20**, 3509–3512.
36 J. N. Solanki and Z. V. P. Murthy, *Ind. Eng. Chem. Res.*, 2011, **50**, 12311–12323.
37 D. Lee, F. R. Michael and R. E. Cohen, *Nano Lett.*, 2006, **6**, 2305–2312.
38 Z. Z. Wu, D. Lee, M. F. Rubner and R. E. Cohen, *Small*, 2007, **3**, 1445–1451.
39 J. F. Bertone, P. Jiang, K. S. Hwang, D. M. Mittleman and V. L. Colvin, *Phys. Rev. Lett.*, 1999, **83**, 300–303.
40 Z. H. Wang, J. H. Zhang, J. Xie, C. Li, Y. F. Li, S. Liang, Z. C. Tian, T. Q. Wang, H. Zhang, H. B. Li, W. Q. Xu and B. Yang, *Adv. Funct. Mater.*, 2010, **20**, 3784–3790.
41 F. M. Hinterholzinger, A. Ranft, J. M. Feckl, B. Rühle, T. Bein and B. V. Lotsch, *J. Mater. Chem.*, 2012, **22**, 10356–10362.
42 C. M. Hansen, *Ind. Eng. Chem. Res.*, 1969, **8**, 2–11.
43 K. Ueno, T. Fukai, T. Nagatsuka, T. Yasuda and M. Watanabe, *Langmuir*, 2014, **30**, 3228–3235.
44 S. Jiang, T. Y. Huang, K. M. Wang, B. Z. Tang and Q. Yu, *Molecules*, 2016, **22**, 54–59.
45 F. Wang, T. J. Threatt and F. M. Vargas, *Fluid Phase Equilib.*, 2016, **430**, 19–32.
46 Y. Fan, J. J. Walish, S. C. Tang, B. D. Olsen and E. L. Thomas, *Macromolecules*, 2014, **47**, 1130–1136.
47 Y. L. Yu, B. D. Kieviet, E. Kutnyanszky, G. J. Vancso and S. D. Beer, *ACS Macro Lett.*, 2015, **4**, 75–79.
48 M. L. Huggins, *Ann. N. Y. Acad. Sci.*, 1942, **43**, 1–32.
49 P. J. Flory, *J. Chem. Phys.*, 1942, **10**, 51–61.
50 S. M. Lee and Y. C. Bae, *Polymer*, 2014, **55**, 4684–4692.
51 F. Ikkai, N. Masui, T. Karino, S. Naito, K. Kurita and M. Shibayama, *Langmuir*, 2003, **19**, 2568–2574.